Pseudogap formation in organic superconductors

Shusaku Imajo [1,*] Takuya Kobayashi [2] Yuki Matsumura,[3] Taiki Maeda,[3] Yasuhiro Nakazawa,[3]
Hiromi Taniguchi,[2] and Koichi Kindo[1]

[1]*Institute for Solid State Physics, University of Tokyo, Kashiwa, Chiba 277-8581, Japan*
[2]*Graduate School of Science and Engineering, Saitama University, Saitama 338-8570, Japan*
[3]*Graduate School of Science, Osaka University, Osaka 560-0043, Japan*

The condensation of paired fermions into superfluid states changes progressively depending on the coupling strength. At the midpoint of the crossover between Bardeen-Cooper-Schrieffer (BCS) weak-coupling and Bose-Einstein condensate (BEC) strong-coupling limits, paired fermions condensate most robustly, thereby leading to the emergence of a pseudogap due to enhanced pairing fluctuations. In the case of electrons in solids, excessively strong interactions often induce competing electronic orders instead of strong-coupling superconductivity, and experimental comprehension of the pseudogap remains incomplete. In this study, we provide experimental evidence demonstrating the opening of a pseudogap, marking the incipient stage of the BCS-BEC crossover in the organic system κ-(BEDT-TTF)$_2 X$. By controlling electron correlations, we investigate the thermodynamic properties of the BCS-BEC crossover and pseudogap phase. Since the superconductivity of κ-(BEDT-TTF)$_2 X$ arises from a simple Fermi liquid that does not exhibit any other electronic orders, our study sheds light on the inherent nature of the BCS-BEC crossover.

I. INTRODUCTION

According to the well-established Bardeen-Cooper-Schrieffer (BCS) theory, fermions undergo the formation of weakly coupled Cooper pairs below a critical temperature T_c. On the other hand, Bose-Einstein condensate (BEC) is a quantum phenomenon observed in bosonic systems, where bosons condensate into the lowest-energy state as a result of the overlap of their wave functions at low temperatures. When the pairing interactions between fermions are enhanced and the pairing deviates from the weak-coupling BCS regime, paired fermions can be regarded as a boson. In such case, fermion pairing into bosons occurs at T^* (greater than T_c), and subsequently, depending on the phase stiffness of the superfluid, the system exhibits the BEC state below T_c. The continuous crossover phenomenon from the weak-coupling BCS regime to the strong-coupling BEC regime is known as the BCS-BEC crossover [1–8]. Experimental investigations of the BCS-BEC crossover have been predominantly conducted in ultracold atomic system, where pairing interactions in a Fermi gas can be controlled through Feshbach resonance [4–7]. For the BCS-BEC crossover of superconductivity in solids, its behavior is modified due to the difference of the kinetic energy associated with the electron motion in a underlying crystal lattice [8]. However, its experimental understanding remains limited due to the difficulty for the significant enhancement of interactions for electron pairing.

Since the BCS-BEC crossover is governed by whether fermion pairs can be viewed as bosons, the spatial size of fermion pairs and the average interfermion distance are principal parameters. In the case of superconducting Cooper pairs, these quantities correspond to the coherence length ξ and the average interelectron distance $1/k_F$ (k_F denotes the Fermi wave number), respectively. The bottom panel of Fig. 1(a) [3,7,8] depicts a schematic phase diagram illustrating the basic behavior of the BCS-BEC crossover. It is important to note that the details of the crossover behavior vary depending on system parameters, such as pairing symmetry and dimensionality [9]. On the BCS side, characterized by a large pair size, the relation $\xi \gg 1/k_F$ holds. In contrast, on the BEC side, where tightly bound fermions are considered as local bosons, the relation $\xi \ll 1/k_F$ applies. In the vicinity of the crossover region, $\xi \sim 1/k_F$ ($k_F \xi \sim 1$), referred to as the unitary regime, the pairs robustly condensate. This results in a peak structure in the heat capacity jump at T_c as a function of $k_F \xi$, as shown in the upper panel of Fig. 1(a) [5,10,11]. Even above T_c, the presence of superfluid fluctuations led to the preformation of Cooper pairs at a pairing temperature T^*, which suppress low-energy single-particle excitations. This is the manifestation of a pseudogap. Various superconductors have been investigated as potential candidates for exploring the BCS-BEC crossover regime [11–16]. However, in low-carrier density systems possessing strong electron correlations, other electronic orderings, or critical phenomena often occur above T_c. Consequently, superconductivity in these systems does not arise from a simple Fermi liquid. To observe a pseudogap, it is essential to observe the suppression of single-particle excitations in the normal state. Therefore, systems with complex electronic states are not ideal for studying the physics of the pseudogap. This difficulty in accurately detecting the pseudogap has hindered detailed discussions regarding the properties of the BCS-BEC in solid-state systems.
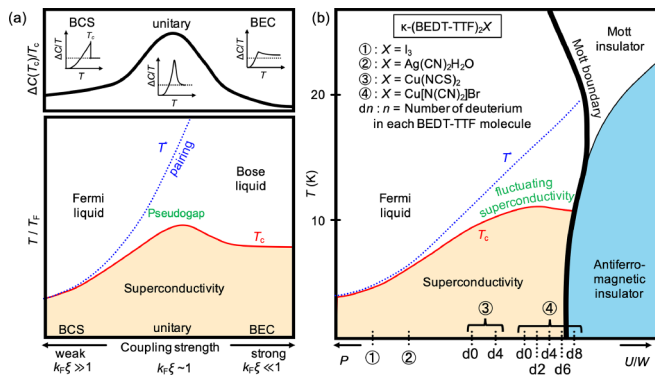
---

*imajo@issp.u-tokyo.ac.jp

FIG. 1. (a) Bottom panel: Schematic of pairing temperature T^* (blue dotted curve) and condensation temperature T_c (red solid curve), both reduced by the Fermi temperature (T_F) as a function of dimensionless coupling strength $k_F\xi$. At the unitary limit, where $k_F\xi$ is of order unity, a pseudogap opens in the temperature range between T_c and T^*. Upper panel: Coupling strength dependence of heat capacity jump at T_c, with schematic $\Delta C/T$ vs T for each limit in the insets. (b) Electronic phase diagram of the half-filled κ-(BEDT-TTF)$_2X$. The κ-type salts with different counter anions X are positioned at different positions on the horizontal axis characterized by pressure/electron correlations. The number n in the expression "dn" stands for the number of deuterium atoms in the ethylene group of each BEDT-TTF molecule.

Half-filled κ-type organic superconductors are strongly correlated systems that exhibit a superconducting transition from a simple Fermi liquid, as shown in Fig. 1(b) [17,18]. When the electron correlation U/W is small (or pressure P is high), the Fermi liquid shows a superconducting transition at low temperatures. An increase in U/W induces band renormalization, leading to enhancement of the effective mass of electrons and T_c. Further increasing U/W causes the ground state to discontinuously become the Mott antiferromagnetic insulator across the first-order Mott phase transition [17,18]. Near the Mott boundary, the value of T_c becomes the maximum, and fluctuating superconductivity was observed in a relatively wide temperature range even above T_c [19–21]. Since these prior studies investigated only strongly correlated (high U/W) salts, the fluctuating superconductivity has been discussed from a perspective of Coulomb penalty associated with the proximity to the Mott boundary. A recent NMR study [22] suggests that the predominant origin of the superconducting fluctuations should be attributable to pseudogap formation. Nevertheless, experimental reports of less correlated (low U/W) salts have been lacking to date, and therefore it has been challenging to ascertain the origin of the fluctuating superconductivity.

In this study, we report that in the κ-type BEDT-TTF system [BEDT-TTF denotes bis(ethylenedithio)-tetrathiafulvalene], the increase in coupling strength pushes toward the unitary regime of the BCS-BEC crossover. We elucidate that the identity of the fluctuating superconductivity observed near the Mott boundary is the pseudogap. Given that the present system is a genuine Fermi liquid showing no other electronic transitions above T_c, our findings demonstrate that the κ-type organic system is a suitable research target for a genuine discussion of the BCS-BEC crossover in strongly correlated

electron systems. We hereafter abbreviate κ-(BEDT-TTF)$_2X$ [$X = $ I$_3$, Ag(CN)$_2$H$_2$O, Cu(NCS)$_2$, and Cu[N(CN)$_2$]Br] as κ-I$_3$, κ-AgCN, κ-NCS, and κ-Br, respectively. The term, dn ($n = 0-8$), represents the number of deuterium atoms present in the ethylene group of each BEDT-TTF molecule. When n is not specified, it indicates that the salt is in its pristine form without any deuteration, namely d0.

II. EXPERIMENTAL METHODS

Single crystals of the κ-type salts were synthesized by electrochemical oxidation methods. Electrical resistance was measured by a standard four-terminal ac method. Torque magnetometry was carried out using a microcantilever. Heat capacity measurements were performed using a customized high-resolution calorimeter with single crystals [23]. To determine H_{c2}, we performed high-field electrical transport measurements using a 60 T pulse magnet.

III. RESULTS

Figures 2(a) and 2(b) present the comparisons of electrical resistivity R and diamagnetic torque dM_z/dH_z as a function of temperature (see the Appendix for a detailed analysis of dM_z/dH_z). Applied fields in the present torque measurements are only a few percent of in-plane H_{c2}, and their impact on T_c is almost negligible. We determine T_c by the onset temperature of the resistance drop. High-resolution torque data can provide information on the emergence of fluctuating superconductivity at T^*. For example, the diamagnetic component of κ-Br appears below $T^* \approx 18.0$ K, which is much higher than $T_c \approx 11.9$ K. The value of $T^* \approx 18.0$ K for κ-Br is consistent with the temperature at which fluctuating superconductivity emerges [19,21,24]. For a full-scale view of the vertical axis, see the Appendix. Similarly, in κ-d6-Br and κ-NCS, T^* observed in this study corresponds to the reported values [19,20,24–26] and is significantly higher than T_c, whereas κ-AgCN and κ-I$_3$ exhibit T^* comparable to T_c. Although fluctuating superconductivity was not observed in κ-NCS in some previous reports [19,22], given the field applied for these measurements and the resolution of the data, these should also be consistent with our present results. Based on the phase diagram shown in Fig. 1(b), these results imply that strong correlations lead to a wider temperature range of fluctuating superconductivity.

Figure 2(c) shows the heat capacity data near T_c for each salt as $\Delta C_{ele}/\gamma T$ versus T/T_c with results reported in Refs. [26–29]. ΔC_{ele} represents the electronic heat capacity difference between the superconducting and normal states, and γ denotes the electronic heat capacity coefficient. Given the resolution of the present data, the heat capacity is not suitable to detect a small fluctuating contribution and determine T^*. Correcting the peak broadened by the fluctuation effect, the height of the jump at T_c in a mean-field approximation $\Delta\gamma/\gamma$ is evaluated as the dashed curves. For a d-wave superconductor in a weak-coupling limit, $2\Delta/k_B T_c \approx 4.3$ yields $\Delta\gamma/\gamma \approx 1.0$ using a gap function $\Delta_0\cos(2\phi)$ in the so-called α model [30]. The salts with smaller U/W exhibit smaller values of $\Delta\gamma/\gamma$, while those with larger U/W show larger values of $\Delta\gamma/\gamma$.
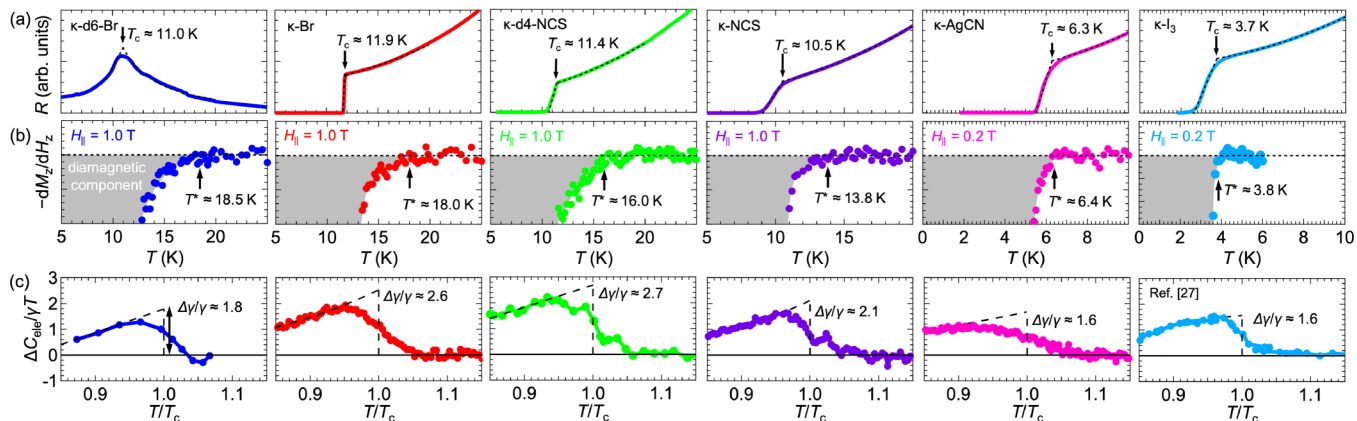
FIG. 2. (a) Resistivity R and (b) diamagnetic susceptibility dM_z/dH_z as a function of temperature. The black arrows in (a) and (b) indicate T_c and T^*, respectively. The gray shaded areas in (b) represent the diamagnetic component. (c) Heat capacity jump $\Delta C_{ele}/\gamma T$ vs reduced temperature T/T_c. The data of κ-I$_3$ are taken from Ref. [27]. The dashed curves are the estimation of mean-field behavior to evaluate the heat capacity jump at T_c, $\Delta\gamma/\gamma$.

IV. DISCUSSION

The present results indicate that fluctuating superconductivity appears in the temperature range between T^* and T_c, which widens in larger U/W salts. We discuss here whether the fluctuating superconductivity corresponds to the formation of the pseudogap. For opening a pseudogap, the system must be situated in the vicinity of the unitary limit. At the unitary limit, the pair condensate is optimally reinforced, and therefore $\Delta\gamma/\gamma$ becomes maximum [10,11,31]. In Fig. 3(a), we show $\Delta\gamma/\gamma$ for each salt with the horizontal axis of
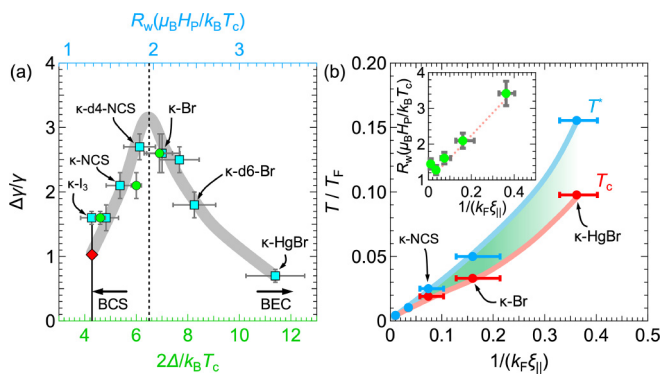

FIG. 3. (a) $\Delta\gamma/\gamma$ vs $2\Delta/k_B T_c$ (bottom axis) and $R_w(\mu_B H_P/k_B T_c)$ (top axis). The blue and green symbols are plotted to the top and bottom axes, respectively. The data of κ-HgBr are taken from Ref. [33]. The solid and dotted lines indicate the positions of the BCS limit ($2\Delta/k_B T_c \approx 4.3$) and the unitary limit ($2\Delta/k_B T_c \approx 6.5$), respectively. The red diamond signifies the calculated value in the framework of the α model [30] using a simple weak-coupling d-wave gap function $\Delta_0 \cos(2\phi)$, where $\Delta_0 = 2.14 k_B T_c$ ($2\Delta/k_B T_c \approx 4.3$). The gray curve is a visual guide. (b) $1/k_F\xi_\parallel$ dependence of T^*/T_F (blue) and T_c/T_F (red). The green shaded area corresponds to the pseudogap region. The inset shows the relation between $R_w(\mu_B H_P/k_B T_c)$ and $1/k_F\xi_\parallel$.

the coupling strength, $2\Delta/k_B T_c$ [27–29,32] for the bottom axis. We plot here the results of prior reports for non-half-filled κ-type salt κ-(BEDT-TTF)$_4$Hg$_{2.89}$Br$_8$ (κ-HgBr) [33], which will be discussed in detail later. As the top axis, $R_w(\mu_B H_P/k_B T_c)$ is also shown in this plot, where R_w, μ_B, and H_P represent Wilson's ratio, the Bohr magneton, and the Pauli limit field, respectively. The values of R_w and H_P are taken from Refs. [25,28,29,34,35] or determined by the high-field transport shown in the Appendix. Since H_P in correlated superconductors is determined by Δ and R_w [25,35,36], $R_w(\mu_B H_P/k_B T_c)$ is proportional to the coupling strength. This plot indicates that $\Delta\gamma/\gamma$ shows a maximum value around $2\Delta/k_B T_c = 6$–7. The value of $2\Delta/k_B T_c \approx 6.5$ was recently proposed as the magic gap ratio, which can be a thermodynamic indicator of the BCS-BEC crossover that is universally observed in various superconductors [11]. This consistency suggests that the unitary region in the κ-type system also lies close to $2\Delta/k_B T_c = 6$–7, and that the larger U/W salts in proximity to the unitary region exhibit a pseudogap phase above T_c.

Although the agreement with the results of the prior studies suggests the BCS-BEC scenario, we must remember that there is much controversy about the presence of the BCS-BEC crossover in cuprates [11,37,38]. To justify the BCS-BEC scenario in the organic salts, it is crucial to demonstrate that the superconducting phase diagram can be explained by a BCS-BEC crossover phase diagram characterized by $1/(k_F\xi)$. In Fig. 3(b), we show T_c (red) and T^* (blue) on the T/T_F versus $1/(k_F\xi_\parallel)$ plot. T_F and $\xi_\parallel$ denote the Fermi temperature and in-plane coherence length, respectively. The values of T_F and $\xi_\parallel$ are calculated by the superfluid density, heat capacity, and H_{c2} data taken from Refs. [27–29,33,39,40]. The inset shows $R_w(\mu_B H_P/k_B T_c)$ versus $1/(k_F\xi_\parallel)$. The positive correlation identifies the relationship between the coupling strength and $1/(k_F\xi_\parallel)$ [10]. Figure 3(b) indicates that the value of $1/(k_F\xi_\parallel)$ for κ-Br is approximately 0.16, which appears smaller than 1 for the unitary regime but not negligible. In the BCS-BEC framework, T_c/T_F is approximately 0.2 in the
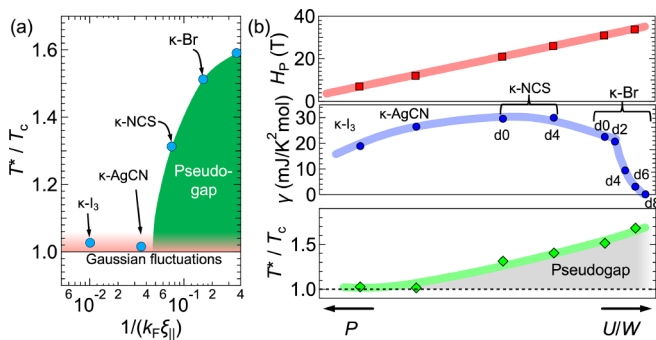
FIG. 4. (a) Evolution of the ratio T^*/T_c depending on $1/k_F\xi_\parallel$. The Gaussian-fluctuation region (red shaded area) is limited to only $T^*/T_c \approx 1.05-1.1$ or less, while the pseudogap phase (green area) covers the higher-temperature region even above $T^*/T_c > 1.1$ when $1/(k_F\xi_\parallel) > 0.05$. (b) Schematic U/W dependence of H_P (top), γ (middle), and T^*/T_c (bottom) of κ-type salts. The curves are visual guides.

BEC side. However, in the case of κ-Br, $T_c/T_F \sim 0.03$, which is much smaller than 0.2. It is worth noting that the BCS-BEC phase diagram of Fermi gases differs slightly from that of superconductors due to the kinetic energy degrees of freedom associated with the electron motion in a periodic lattice. For two-dimensional superconductors, T_c/T_F in the BEC limit decreases and approaches approximately 1/8 [41]. Moreover, T_c/T_F depends on the effective mass of fermions and pairing symmetry. In cases in which the effective mass becomes heavier or the symmetry is d-wave, changes in the BCS-BEC phase diagram, such as a decrease in T_c/T_F, occur [3,7,8]. Given the d-wave superconducting state and the strongly renormalized effective mass due to large U/W in κ-Br, $T_c/T_F \sim 0.03$ is reasonable. In the case of Li$_x$ZrNCl gate-controlled layered superconductors [15], pseudogap formation occurs when the Li content x is below 0.05. At $x \approx 0.05$, the values of $1/(k_F\xi) \approx 0.1$ and $T_c/T_F \approx 0.05$ yield $T^*/T_c \approx 1.5$. These values are consistent with the results obtained for κ-Br, which suggests that fluctuating superconductivity in the κ-type system can also be identified as a pseudogap phase.

We note that the superconducting properties of κ-HgBr [$1/(k_F\xi_\parallel) = 0.3-0.4$ and $T_c/T_F \approx 0.1$] [16,42] can also be explained in the framework expected from extrapolations of κ-Br and κ-NCS. κ-HgBr has been considered as a unique salt that does not share the same electronic phase diagram as Fig. 1(b) due to its distinct features, such as band filling deviating from half and quantum-spin-liquid-like behavior [42]. The previous studies [16,42] have discussed the BCS-BEC crossover of κ-HgBr as distinct from superconducting properties of half-filled κ-type salts. However, the present results demonstrate that κ-HgBr also shares the same superconducting phase diagram as the other κ-type superconducting state from the perspective of the BCS-BEC physics.

These considerations unveil the BCS-BEC physics in the κ-type superconductors. Nevertheless, we need to evaluate the effect of thermal fluctuations on the present superconductivity. To make the fluctuating region clearer, in Fig. 4(a) we show

T^*/T_c versus $1/(k_F\xi_\parallel)$ as a semilogarithmic plot. In the classical framework, order parameters are fluctuated by thermal energy, and the behavior in the critical region is described by Gaussian fluctuations. The Gaussian critical region T_G/T_c is estimated by the equation $T_G/T_c = 1 + 2(k_B/8\pi \Delta C \xi^3)^2$, where ΔC denotes heat capacity jump at T_c [43]. T_G/T_c for the present κ-type salts is in the range of 1.05–1.1, which corresponds to the broadened region of the heat capacity data shown in Fig. 2(c). Nevertheless, it is hard to reconcile the Gaussian-fluctuation region with the value of T^*/T_c when $1/(k_F\xi_\parallel) > 0.05$, as shown in Fig. 4(a). Therefore, the wide fluctuating region for larger U/W salts originates from the formation of a pseudogap.

Finally, we consider the electron-correlation dependence of κ-type superconductivity. The exact calculation of the values of low-temperature U/W is challenging due to the lack of the structural data at low temperatures near T_c. To estimate the relative magnitude of U/W roughly, we use H_P, which is strongly influenced by U/W. In the top panel of Fig. 4(b), we show the relative positions of the measured salts to make the U/W dependence of H_P linear in this plot. Long-standing experimental studies [17,18] have established the U/W dependence of γ, as shown in the middle panel of Fig. 4(b). In the low U/W region, γ increases with increasing U/W. This behavior can be understood within the Brinkman-Rice framework [44], which suggests that electron correlations result in the renormalization of the electron mass. However, in the immediate vicinity of the Mott boundary, a significant reduction in γ is observed for κ-dn-Br ($n = 4-8$) [18,26]. This is because the Mott transition is first-order, and the normal state is eroded with the insulating state by inhomogeneity, leading to the reduction in γ. Therefore, the abrupt drop in γ should not relate to the BCS-BEC crossover. On the other hand, the gradual change in γ, observed in the region where the pseudogap opens [Figs. 4(b) and 4(c)], might be caused by pairing fluctuations in the normal state in the BEC region [11,31]. To understand the influence of the BCS-BEC crossover on the normal state, further future studies are required.

V. CONCLUSION AND PERSPECTIVE

Our comprehensive investigation of the superconducting state in the κ-type organic system revealed the formation of a pseudogap near the unitary limit through the tuning of electron correlations. Given that the normal state of the κ-type salts is a simple Fermi liquid without any other electronic ordering, the present findings are crucial for identifying the essential parameters required to gain an accurate understanding of BCS-BEC physics. It is worth noting that the crossover behavior of this system can be controlled through external pressure. Hence, it is desirable to conduct detailed high-pressure studies of the κ-type system that focus on the pseudogap in the future.
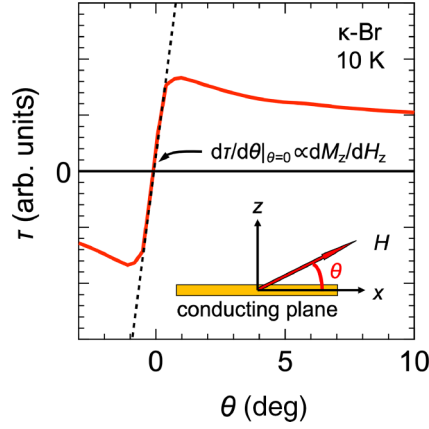
FIG. 5. A typical example of the angle dependence of magnetic torque for κ-type superconductors. The inset illustrates the definition of angle and direction in the present measurements.

APPENDIX

1. Evaluation of the diamagnetic signal derived from magnetic torque measurements

In Fig. 2 of the main text, we present the temperature dependence of the perpendicular component of the diamagnetic susceptibility of superconductivity, dM_z/dH_z. To obtain dM_z/dH_z, we employed angle-resolved magnetic torque measurements using microcantilevers. As shown in Fig. 5, we measured the angle-dependent torque of each sample in a magnetic field at various temperatures. The inset displays a schematic of the sample setup for the measurements, with the direction parallel to the in-plane direction set as 0 deg. In the angle range of ± 0.5 deg, the torque signal can be described by the following formula:

$$
\begin{aligned}
\frac{d\tau}{d\theta}\Big|_{\theta=0} &= -\mu_0 H_x \frac{d(M \times H)}{dH_z}\Big|_{\theta=0} \\
&= \mu_0 H_x \frac{d(H_x M_z - M_x H_z)}{dH_z}\Big|_{\theta=0} \\
&= \mu_0 H_x \frac{d[H_x H_z(M_z/H_z - M_x/H_x)]}{dH_z}\Big|_{\theta=0}.
\end{aligned} \tag{A1}
$$

Here, we use the relations $H_x = H\cos\theta$ and $H_z = H\sin\theta$. In the mixed state of two-dimensional superconductors, since $|M_z/H_z|$ is much larger than $|M_x/H_x|$ in this angle range, the
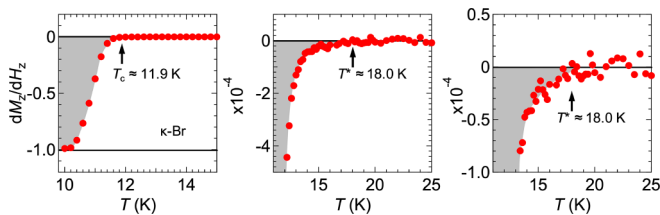

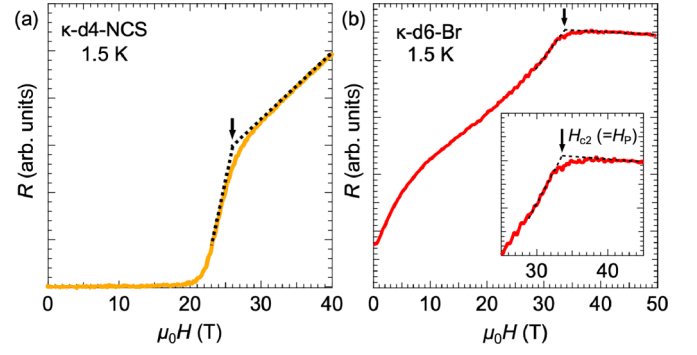FIG. 6. Temperature dependence of dM_z/dH_z of κ-Br. Shaded areas indicate the diamagnetic component.

formula can be rewritten as

$$
\frac{d\tau}{d\theta}\Big|_{\theta=0} \approx -\mu_0 H_x^2 \frac{dM_z}{dH_z}\Big|_{\theta=0} \propto \frac{dM_z}{dH_z}\Big|_{\theta=0} \tag{A2}
$$

in a constant field. Therefore, the slope of the angle-dependent torque near the in-plane configuration is proportional to the perpendicular component of the diamagnetic susceptibility of superconductivity.

2. Temperature dependence of dM_z/dH_z

In Fig. 2(b) in the main text, we show enlarged plots of dM_z/dH_z to emphasize the emergence of the diamagnetic component below T^*. In Fig. 6, we plot dM_z/dH_z versus T of κ-Br at various scales. From the left full-scale view, the onset temperature of the emergence of the diamagnetic component appears to be more T_c than T^*, which corresponds to the resistivity data shown in Fig. 2(a). Nevertheless, from the center and right figures, which are enlargements of the left figure, we can find that the diamagnetic component is present even above T_c, as discussed in the main text. Thus, the fluctuation (pseudogap) region between T_c and T^* can be determined from the difference between the resistivity and torque data, respectively.

3. High-field measurement for determining H_{c2}

In the main text, we evaluate the coupling strength using the dimensionless ratio $R_w(\mu_B H_P/k_B T_c)$, as shown in Fig. 3(a), as H_P in correlated superconductors is determined by Δ and R_w [35,36]. For κ-Br, κ-NCS, κ-AgCN, κ-I$_3$, and κ-HgBr, H_P was reported in Refs. [25,28,29,33,34]. In this study, we obtained H_P of κ-d4-NCS and κ-d6-Br using a high-field transport measurement with a 60 T pulse magnet. Figure 7 displays the in-plane magnetic field dependence of the electrical resistance of κ-d4-NCS and κ-d6-Br at 1.5 K. In the case of these salts, H_P corresponds to H_{c2}, as the orbital pair breaking effect is quenched when a field is applied parallel to the two-dimensional conducting plane. Since we determine T_c from the onset of the resistance drop, as shown in Fig. 2(a), H_{c2} is also determined by the onset position indicated by the arrow.

FIG. 7. Magnetoresistance of (a) κ-d4-NCS and (b) κ-d6-Br in an in-plane field at 1.5 K. Arrow indicates H_{c2}, which corresponds to H_P. The inset of (b) shows an enlarged view around H_{c2}.

[1] D. M. Eagles, Possible pairing without superconductivity at low carrier concentrations in bulk and thin-film superconducting semiconductors, Phys. Rev. **186**, 456 (1969).

[2] M. Drechsler and W. Zwerger, Crossover from BCS-superconductivity to Bose-condensation, Ann. Phys. (Berlin) **504**, 15 (1992).

[3] C. A. R. Sá de Melo, M. Randeria, and J. R. Engelbrecht, Crossover from BCS to Bose superconductivity: Transition temperature and time-dependent Ginzburg-Landau Theory, Phys. Rev. Lett. **71**, 3202 (1993).

[4] S. Jochim, M. Bartenstein, A. Altmeyer, G. Hendl, S. Riedl, C. Chin, J. H. Denschlag, and R. Grimm, Bose-Einstein condensation of molecules, Science **302**, 2101 (2003).

[5] M. W. Zwierlein, C. A. Stan, C. H. Schunck, S. M. F. Raupach, S. Gupta, Z. Hadzibabic, and W. Ketterle, Observation of Bose-Einstein condensation of molecules, Phys. Rev. Lett. **91**, 250401 (2003).

[6] J. P. Gaebler, J. T. Stewart, T. E. Drake, D. S. Jin, A. Perali, P. Pieri, and G. C. Strinati, Observation of pseudogap behaviour in a strongly interacting Fermi gas, Nat. Phys. **6**, 569 (2010).

[7] M. Randeria and E. Taylor, Crossover from Bardeen-Cooper-Schrieffer to Bose-Einstein condensation and the unitary Fermi gas, Annu. Rev. Condens. Matter Phys. **5**, 209 (2014).

[8] Q. Chen, Z. Wang, R. Boyack, S. Yang, and K. Levin, When superconductivity crosses over: From BCS to BEC, arXiv:2208.01774.

[9] Q. Chen, I. Kosztin, B. Jankó, and K. Levin, Superconducting transitions from the pseudogap state: d-wave symmetry, lattice, and low-dimensional effects, Phys. Rev. B **59**, 7083 (1999).

[10] R. Haussmann, W. Rantner, S. Cerrito, and W. Zwerger, Thermodynamics of the BCS-BEC crossover, Phys. Rev. A **75**, 023610 (2007).

[11] N. Harrison and M. K. Chan, Magic gap ratio for optimally robust fermionic condensation and its implications for high-T_c superconductivity, Phys. Rev. Lett. **129**, 017001 (2022).

[12] T. Timusk and B. Statt, The pseudogap in high-temperature superconductors: an experimental survey, Rep. Prog. Phys. **62**, 61 (1999).

[13] S. Kasahara, T. Yamashita, A. Shi, R. Kobayashi, Y. Shimoyama, T. Watashige, K. Ishida, T. Terashima, T. Wolf, F. Hardy, C. Meingast, H. v. Löhneysen, A. Levchenko, T. Shibauchi, and Y. Matsuda, Giant superconducting fluctuations in the compensated semimetal FeSe at the BCS-BEC crossover, Nat. Commun. **7**, 12843 (2016).

[14] Y. Cao, V. Fatemi, S. Fang, K. Watanabe, T. Taniguchi, E. Kaxiras, and P. Jarillo-Herrero, Unconventional superconductivity in magic-angle graphene superlattices, Nature (London) **556**, 43 (2018).

[15] Y. Nakagawa, Y. Kasahara, T. Nomoto, R. Arita, T. Nojima, and Y. Iwasa, Gate-controlled BCS-BEC crossover in a two-dimensional superconductor, Science **372**, 190 (2021).

[16] Y. Suzuki, K. Wakamatsu, J. Ibuka, H. Oike, T. Fujii, K. Miyagawa, H. Taniguchi, and K. Kanoda, Mott-Driven BEC-BCS crossover in a doped spin liquid candidate κ-(BEDT-TTF)$_4$Hg$_{2.89}$Br$_8$, Phys. Rev. X **12**, 011016 (2022).

[17] K. Kanoda, Metal-insulator transition in κ-(ET)$_2 X$ and (DCNQI)$_2 M$: Two contrasting manifestation of electron correlation, J. Phys. Soc. Jpn. **75**, 051007 (2006).

[18] Y. Nakazawa, S. Imajo, Y. Matsumura, S. Yamashita, and H. Akutsu, Thermodynamic picture of dimer-mott organic superconductors revealed by heat capacity measurements with external and chemical pressure control, Crystals **8**, 143 (2018).

[19] M.-S. Nam, A. Ardavan, S. J. Blundell, and J. A. Schlueter, Fluctuating superconductivity in organic molecular metals close to the Mott transition, Nature (London) **449**, 584 (2007).

[20] S. Tsuchiya, J. Yamada, S. Tanda, K. Ichimura, T. Terashima, N. Kurita, K. Kodama, and S. Uji, Fluctuating superconductivity in the strongly correlated two-dimensional organic superconductor κ-(BEDT − TTF)$_2$Cu(NCS)$_2$ in an in-plane magnetic field, Phys. Rev. B **85**, 220506(R) (2012).

[21] S. Tsuchiya, J. Yamada, T. Terashima, N. Kurita, K. Kodama, K. Sugii, and S. Uji, Fluctuating Superconductivity in the strongly correlated organic superconductor κ-(BEDT-TTF)$_2$Cu[N(CN)$_2$]Br, J. Phys. Soc. Jpn. **82**, 064711 (2013).

[22] T. Furukawa, K. Miyagawa, M. Matsumoto, T. Sasaki, and K. Kanoda, Microscopic evidence for preformed Cooper pairs in pressure-tuned organic superconductors near the Mott transition, Phys. Rev. Res. **5**, 023165 (2023).

[23] S. Imajo, S. Fukuoka, S. Yamashita, and Y. Nakazawa, Construction of relaxation calorimetry for 10^{1-2} µg samples and heat capacity measurements of organic complexes, J. Therm. Anal. Calorim. **123**, 1871 (2016).

[24] M. Dion, D. Fournier, M. Poirier, K. D. Truong, and A.-M. S. Tremblay, Mixed pairing symmetry in κ-(BEDT-TTF)$_2 X$ organic superconductors from ultrasonic velocity measurements, Phys. Rev. B **80**, 220511(R) (2009).

[25] S. Imajo, T. Nomura, Y. Kohama, and K. Kindo, Emergent anisotropy in the Fulde-Ferrell-Larkin-Ovchinnikov state, Nat. Commun. **13**, 5590 (2022).

[26] Y. Matsumura, S. Imajo, S. Yamashita, H. Akutsu, and Y. Nakazawa, Electronic heat capacity and lattice softening of partially deuterated compounds of κ-(BEDT-TTF)$_2$Cu[N(CN)$_2$]Br, Crystals **12**, 2 (2022).

[27] J. Wosnitza, X. Liu, D. Schweitzer, and H. J. Keller, Specific heat of the organic superconductor κ-(BEDT-TTF)$_2$I$_3$, Phys. Rev. B **50**, 12747 (1994).

[28] S. Imajo, Y. Nakazawa, and K. Kindo, Superconducting Phase Diagram of the Organic Superconductor κ-(BEDT-TTF)$_2$Cu[N(CN)$_2$] above 30 T, J. Phys. Soc. Jpn. **87**, 123704 (2018).

[29] S. Imajo, K. Kindo, and Y. Nakazawa, Symmetry change of d-wave superconductivity in κ-type organic superconductors, Phys. Rev. B **103**, L060508 (2021).

[30] H. Padamsee, J. E. Neighbor, and C. A. Shiffman, Quasiparticle phenomenology for thermodynamics of strong-coupling superconductors, J. Low Temp. Phys. **12**, 387 (1973).

[31] P. van Wyk, H. Tajima, R. Hanai, and Y. Ohashi, Specific heat and effects of pairing fluctuations in the BCS-BEC crossover regime of an ultracold Fermi gas, Phys. Rev. A **93**, 013621 (2016).

[32] O. J. Taylor, A. Carrington, and J. A. Schlueter, Specific-heat measurements of the gap structure of the organic superconductors κ-(ET)$_2$Cu[N(CN)$_2$]Br and κ-(ET)$_2$Cu(NCS)$_2$, Phys. Rev. Lett. **99**, 057001 (2007).

[33] S. Imajo, S. Sugiura, H. Akutsu, Y. Kohama, T. Isono, T. Terashima, K. Kindo, S. Uji, and Y. Nakazawa, Extraordinary π-electron superconductivity emerging from a quantum spin liquid, Phys. Rev. Res. **3**, 033026 (2021).

[34] S. Wanka, D. Beckmann, J. Wosnitza, E. Balthes, D. Schweitzer, W. Strunz, and H. J. Keller, Critical fields and mixed-state properties of the layered organic superconductor κ-(BEDT-TTF)$_2$I$_3$, Phys. Rev. B **53**, 9301 (1996).

[35] R. H. McKenzie, Wilson's ratio and the spin splitting of magnetic oscillations in quasi-two-dimensional metals, arXiv:cond-mat/9905044.

[36] C. C. Agosta, Inhomogeneous superconductivity in organic and related superconductors, Crystals **8**, 285 (2018).

[37] J. L. Tallon, Comment on "Magic Gap Ratio for Optimally Robust Fermionic Condensation and Its Implications for High-T_c Superconductivity," Phys. Rev. Lett. **130**, 199701 (2023).

[38] J. Sous, Y. He, and S. A. Kivelson, Absence of a BCS-BEC crossover in the cuprate superconductors, npj Quantum Mater. **8**, 25 (2023).

[39] K. Wakamatsu, K. Miyagawa, and K. Kanoda, Superfluid density versus transition temperature in a layered organic superconductor $\kappa-$(BEDT-TTF)$_2$Cu[N(CN)$_2$]Br under pressure, Phys. Rev. Res. **2**, 043008 (2020).

[40] N. Yoneyama, A. Higashihara, T. Sasaki, T. Nojima, and N. Kobayashi, Impurity effect on the in-plane penetration depth of the organic superconductors κ-(BEDT-TTF)$_2$X (X = Cu(NCS)$_2$ and Cu[N(CN)$_2$]Br), J. Phys. Soc. Jpn. **73**, 1290 (2004).

[41] T. Hazra, N. Verma, and M. Randeria, Bounds on the superconducting transition temperature: Applications to twisted bilayer graphene and cold atoms, Phys. Rev. X **9**, 031049 (2019).

[42] H. Oike, Y. Suzuki, H. Taniguchi, Y. Seki, K. Miyagawa, and K. Kanoda, Anomalous metallic behaviour in the doped spin liquid candidate κ-(ET)$_4$Hg$_{2.89}$Br$_8$, Nat. Commun. **8**, 756 (2017).

[43] K. F. Quader and E. Abrahams, Superconducting fluctuations in specific heat in a magnetic field: Dimensional crossover, Phys. Rev. B **38**, 11977 (1988).

[44] W. F. Brinkman and T. M. Rice, Application of gutzwiller's variational method to the metal-insulator transition, Phys. Rev. B **2**, 4302 (1970).